Leaky-Wave Slot Array Antenna Fed by a Dual Reflector System

Mauro Ettorre, *Member, IEEE*, Andrea Neto, *Member, IEEE*, Giampiero Gerini, *Senior Member, IEEE*, and Stefano Maci, *Fellow, IEEE*

***Abstract*—A leaky-wave slot array antenna fed by a dual offset Gregorian reflector system is realized by pins in a parallel plate waveguide. The radiating part of the antenna is composed by parallel slots etched on one side of the same parallel plate waveguide. The dual offset Gregorian reflector system is fed by an arrangement constituted by two vias and a grid, also constituted by pins. Also this feed arrangement realizes a leaky type of radiation, this time inside the parallel plate waveguide. A prototype of the antenna has been designed, manufactured and successfully tested. The low profile, low cost and high efficiency of the antenna render it suited for a variety of radar or telecom applications.**

***Index Terms*—Leaky-wave antennas (LWA), millimeter-wave antennas, planar antennas, reflector antennas.**

I. Introduction

PLANAR leaky-wave antennas (LWAs) have received much attention in the recent years for applications in the millimeter-wave ranges. In particular the compatibility with printed circuit board technology (PCB) and the low profile are the strongest features of these antennas. Planar LWAs can be categorized in different topologies depending on the geometry of the structure and on the kind of traveling wave mode [1], [2]. In particular the nature of the traveling wave mode classifies mono and two-dimensional leaky-wave antennas. These classifications have a direct implication on the type of beam, that however maintains the typical scanning behavior versus frequency.

Mono dimensional planar leaky-wave antennas are characterized by a fan beam; then, array solutions or two-dimensional planar leaky-wave antennas are needed to radiate a pencil beam.

An array solution of mono dimensional planar leaky-wave antennas would have the disadvantages of a cumbersome feeding network accompanied by a probable low efficiency. On the other hand two-dimensional leaky-wave antennas have the advantage of absence of the feeding network, but they are less flexible for beam shaped designing.

The pencil beam leaky-wave antenna presented here, an array of slots etched on one plate of a parallel plate waveguide (PPW), is fed by a dual offset Gregorian reflector system realized by vias connecting the two plates of the PPW. The antenna is shown in Fig. 1.

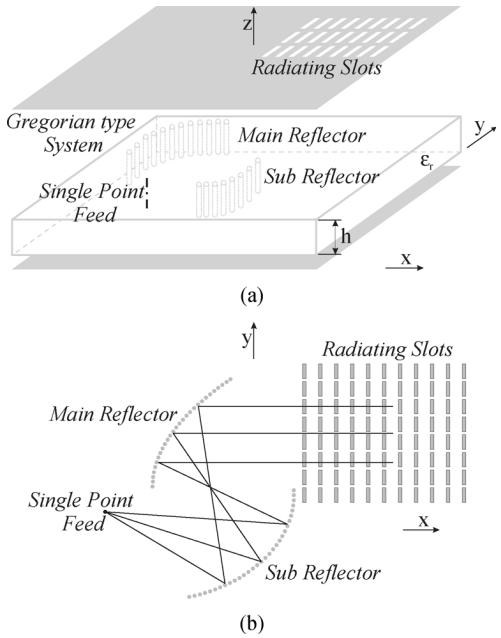

Fig. 1. (a) 3-D view of the antenna. The dual reflector feed system is made by pins connecting the two plates of the parallel plate waveguide. (b) Top view of the antenna.

This antenna could be classified as a periodic one-dimensional slot array leaky-wave antenna. A probe-type source has been used to feed the Gregorian system. This arrangement is suited to printed circuit board fabrication processes. Furthermore it has the advantage to avoid a beam forming network while preserving the freedom to shape the amplitude of the plane feeding wavefront. The azimuth and elevation plane of the slot array can be thus shaped independently by acting on the focal plane feeding of the Gregorian system and on the parameters of the leaky-wave radiating slots. This leads various degrees of freedom in the design. In particular a frequency reuse scheme renders possible the scanning in the E-plane, while a multi-feed focal plane renders possible the scanning in the H-plane. Overall this solution opens possibilities for those applications that are right now implemented with 3-D focusing imaging-like systems.

Manuscript received February 12, 2008; revised June 16, 2008. Current version published October 3, 2008.

M. Ettorre was with TNO Defence, Safety and Security, Den Haag 2597 AK, The Netherlands. He is now with the Groupe Antennes and Hyperfréquences, Institut d'Electronique et de Télécommunications de Rennes (IETR), UMR CNRS 6164, Université de Rennes 1, 35042 Rennes Cedex, France (e-mail: mauro.ettorre@univ-rennes1.fr).

A. Neto and G. Gerini are with TNO Defence, Safety and Security, Den Haag 2597 AK, The Netherlands (e-mail: andrea.neto@tno.nl; giampiero.gerini@tno.nl).

S. Maci is with the Department of Information Engineering, University of Siena, 53100 Siena, Italy. (e-mail: macis@dii.unisi.it.

Color versions of one or more of the figures in this paper are available online at http://ieeexplore.ieee.org.

Digital Object Identifier 10.1109/TAP.2008.929457

TABLE I
PARAMETERS OF THE DUAL OFFSET GREGORIAN SYSTEM IN TERMS OF THE FREE SPACE WAVELENGTH λ

D	d_0	F_m	F_{eq}	e	$2C$	M	$\lvert\alpha\rvert$	β
5.67λ	2.96λ	2.49λ	5.3λ	0.4	4.68λ	2.13	38.56°	17.06°

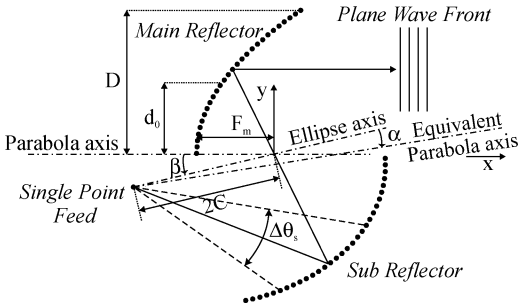

Fig. 2. Geometry of the dual offset reflector system made by pins in PPW.

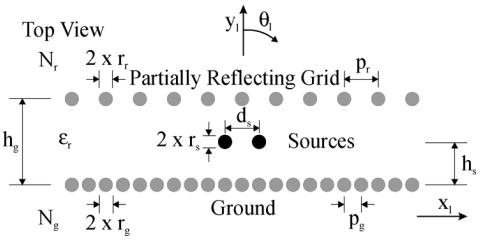

Fig. 3. Pin-made feed geometry. The pins connect the upper and lower wall of the parallel plate waveguide. The center of the reference system $x_l - y_l$ corresponds to the feed point of Fig. 2 and the y_l axis is oriented along the equivalent parabola axis.

The paper is organized as follows. In Section II the 2-D Gregorian system is designed by resorting to a geometrical optics (GO) tracing of the rays associated to the dominant PPW transverse electromagnetic (TEM) mode. In Section III a pin-made feed for the dual reflector system (more detailed than the one indicated in Fig. 1) is presented; this feed allows the improvement of the spill-over efficiency of the Gregorian system. In Section IV, simplified formulas are derived and used to design the radiating slot array. Section V presents experimental results for a prototype. Section VI concludes outlining future applications and development of the present antenna.

II. DUAL OFFSET REFLECTOR GREGORIAN SYSTEM MADE BY PINS

The power distribution required to feed the slot array is achieved by resorting to quasi-optics concepts. As already mentioned, the convenience to operate with printed circuit board technology suggests to implement the reflectors by means of vertical metallic pins. The geometry of the proposed reflector system is shown in Fig. 2.

The distance between contiguous pins is less than 1/20 of the dielectric wavelength, $\lambda_m = \lambda/\sqrt{\epsilon_r}$, at the central operating frequency. Note that $\epsilon_r = 2.2$ will be justified in Section IV. The thickness of the pins is of minor importance. A compactness requirement imposes a dual reflector system and an offset configuration is chosen to avoid the blockage from the feed. The chosen Gregorian configuration allows a good efficiency, for a given volume, while adding the degree of freedom to shape the plane wavefront amplitude tapering once the feed is fixed. To compensate for the asymmetry of the dual offset reflector, the Mizugutch's condition is used, that ensures good symmetry of the plane wave front and good scan capability [3], [4]. Since the design is a simple two-dimensional version of a classic three dimensional Gregorian configuration, it is not described here in depth. More details can be found in [5], [6]. We will just mention that a Gregorian reflector is defined by the eccentricity e of the ellipse that hosts on its first and second focus the feed and the focal point of the main reflector. A Gregorian reflector is also characterized by a main parabola and an equivalent parabola that are not necessarily parallel. In practice the Mizugutch's condition is given by

$$\tan(\alpha) = \frac{|1-e^2|\sin(\beta)}{(1+e^2)\cos(\beta) - 2e} \tag{1}$$

where α is the angle between the ellipse and the equivalent parabola main axes and β is the angle between the parabola and the ellipse main axes (see Fig. 2). It is worth noting that in this case the magnification ratio [i.e., the ratio between the equivalent focal length (F_{eq}) and the main reflector parabola focal length (F_m)] is given by

$$M = \frac{|1-e^2|}{(1+e^2) - 2e\cos(\beta)}. \tag{2}$$

The principal geometry parameters characterizing the dual offset reflector system are reported in Table I in terms of the free space wavelength λ.

We just underline the fact that we are treating as a bundle of rays the cylindrical TEM wavefront excited by the source, thus obtaining a *quasi*–TEM ($qTEM$) plane wave modulated in amplitude along the planar wave front. This wavefront is used next to feed the slot array.

To completely define a dual offset reflector five parameters have to be fixed and the others can be found using geometric relations. In our case we started the design from $F_m, 2C, e, d_0$ and the feed illumination angle $\Delta\theta_s = 2\theta_l|_{-10\,\mathrm{dB}}$ ($\Delta\theta_s$ is shown in Fig. 2 and θ_l is shown in Fig. 3), that is the $-10\,\mathrm{dB}$ beamwidth corresponding to the level of subreflector tapering adopted. The choice was in practice to start from the geometrical parameters that implied a minimization of volume, while retaining given characteristics, $\Delta\theta_s$, for the feed.

As we will see in the following, a leaky effect is used to shape the feed pattern and then attention has to be taken in a multibeam design in order to reduce the mutual coupling between neighboring feeds. In particular a tradeoff between coupling and directivity of the feed pattern has to be found and reflected in the reflector design through $\Delta\theta_s$.

For our prototype a source illumination angle of $\Delta\theta_s = 50°$ has been chosen to get a system with an equivalent F_{eq}/D of 0.933.

III. Excitation of the Gregorian System

The efficient excitation of reflector feeds has been investigated for decades and is one of the main problems in the antenna field. Recently a strategy has been proposed to excite conventional reflector antennas to achieve either high-efficiency in single feed reflectors [7] or overlapping apertures in multibeam imaging systems [8].

In this case the feed is integrated in the PCB structure and realized via metallic posts just like the reflector, Fig. 3. A leaking mode propagates in a partially reflecting waveguide constituted by two grids of pins. The lower wall of this waveguide is well sampled (N_g pins) and provides the equivalent of a continuous metallization, while the upper wall, being constituted by a larger period (N_r pins), allows a spill-over of energy in the external environment. The two walls are separated by a distance $0.44\lambda/\sqrt{\epsilon_r}$ at the central operating frequency.

To analyze the properties of the structure, one can remove the two metallic walls of the PPW in $z = 0$ and $z = h$ connected by the pins and by repetitive applications of the image principle, the structure results into a 2-D double grid of infinite thin wires excited by two line sources in the middle. In a first order approximation one can imagine that the propagation inside this so obtained double grid structure post wall is a slight alteration of the unperturbed TE_1 mode in a continuous wall parallel plate waveguide. However the mode is a leaky mode (w.r.t the y_l direction) that has a complex propagation constant with a real part close to the one of the unperturbed TE_1 mode and an imaginary attenuation constant associated to radiation losses in the 2-D medium. This mode of propagation is in many aspects similar to the TE/TM leaky modes that were considered in [7] and [8], the key difference being that the radiation now occurs in the PPW structure rather than in free space.

The exact knowledge of the complex propagation constant and its dispersion diagram is essential to shape the feed's pattern. In particular, the pattern can be shaped in order to reduce the spill-over and tapering losses for the dual reflector system.

A home made numerical tool has been developed to obtain the dispersion properties of the structure. The details of the procedure are not given because they are small modifications of the method described in [9] and beyond the goal of the present paper. With the geometrical dimensions given in Table II, Fig. 4 gives the results for a number of test cases with different periodicity (p_r) for the partially reflecting grid. This figure shows the behavior of the real and the imaginary part of the complex propagation constant, normalized to the propagation constant of the $qTEM$ wave in the dielectric $k_m = k_0\sqrt{\epsilon_r}$. The real part of the propagation constant, as the periodicity p_r increases, deviates from that of the TE_1 but it exhibits a smooth variation versus frequency that allows one to achieve a wider bandwidth. The real part of the propagation constant, here, is directly linked to the pointing direction of the leaky wave beam $\theta_l = \arcsin(k_{x_l}/k_m)$ which is indicated in Fig. 3. Note that the pointing angle of the leaky wave defines the portion of the sub reflector where most of the energy is concentrated. The tradeoff

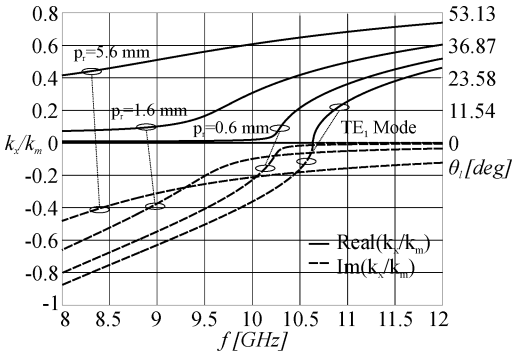

Fig. 4. Dispersion diagram of the pin-made feed for different periods p_r. For comparison, the dispersion characteristics of unperturbed TE_1 mode are also shown. The propagation constants in both cases are normalized to that of the medium k_m.

TABLE II
Geometrical Dimensions in Millimeters of the Pin-Made Feed

h_g	h_s	N_g	N_r	r_g	r_r	r_s	p_g	p_r	d_s
9.5	4.75	157	15	0.15	0.15	0.22	0.5	5.6	12

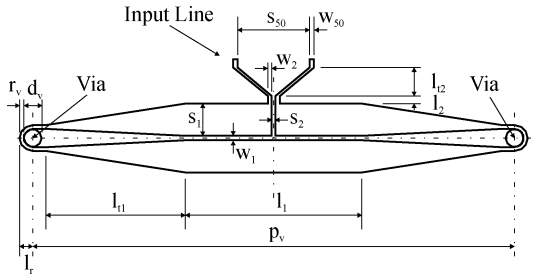

Fig. 5. Geometry of the matching network for the two vias of the feed. The 50 Ohm input line is connected to a SMA connector to measure the antenna prototype.

between phase and amplitude of the desiderated aperture distribution, together with the achievement of a reasonable bandwidth, brings to chose $p_r = 5.6$ mm.

As shown in Figs. 3 and 5, two in-phase fed probes have been used to excite the parallel grid waveguide leaky-mode. The two probes are separated by a distance p_v, that is almost half dielectric wavelength at the central operating frequency and they are fed by a single input 50 Ohm coplanar waveguide. The matching network transforms the original impedances at the vias from 250 Ohm to 50 Ohm at the input line and at the same time it compensates for the inductive loads of the vias. Table III reports the final dimensions of the matching network.

The double probe solution has been preferred to that with a single probe because it leads to an intrinsical narrower beam that allows the use of a flatter curve in Fig. 4, being fixed the requirements of beamwidth. The feed integrated in the antenna prototype has been finally designed to achieve a tapering of -10 dB in correspondence of the sub reflector edges ($\Delta\theta_s = 50°$). The calculated pattern at the central frequency ($f_c = 9.35$GHz) is shown in Fig. 6. Note that only one beam appears even if two leaky-waves aiming at two angles, symmetric with respect to y_l, are originated. This because the two beams are very close one to the other and coalesce. The pattern is normalized with respect to the square-root of the distance from the phase center, being

TABLE III
GEOMETRICAL DIMENSIONS IN MILLIMETERS OF THE MATCHING NETWORK FOR THE PIN-MADE FEED

r_v	d_v	l_r	l_1	l_2	l_{t1}	l_{t2}	p_v	s_1	w_1	s_2	w_2	s_{50}	w_{50}
0.1	0.44	0.325	2.15	0.2	3.475	0.7	12	0.8	0.1	0.1	0.1	1.8	0.1

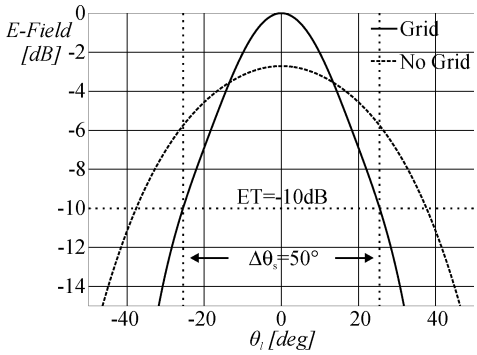

Fig. 6. Normalized amplitude of the cylindrical wave launched in the PPW by the pin-made feed (continuous line) and comparison with the incident field of the feed without upper grid (dashed line).

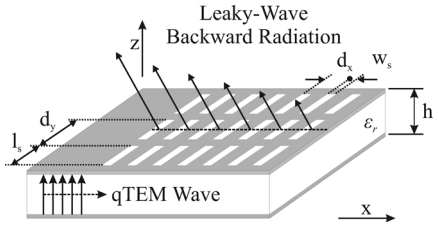

Fig. 7. Geometry of the radiating slots. The slots are etched on the upper plate of the parallel plate waveguide. The periodicity of the slots is such as to have a backward radiation in the operating band.

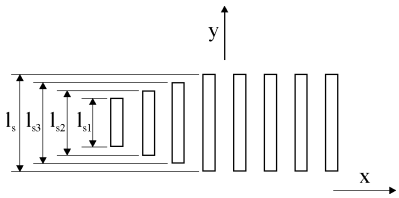

Fig. 8. Detail of the transition from PPW to radiating slots.

the field relevant to a cylindrical $qTEM$ wave into the PPW. For comparison also the feed pattern that would be obtained with the backing reflector grid but without the partially reflecting grid, is shown.

IV. DISPERSION ANALYSIS OF THE SLOT ARRAY

The radiating part of the system is composed by an array of slots etched on the upper plate of a parallel plate waveguide structure, operating in a backward leaky-wave mode.

The geometric parameters of the slots used in our antenna prototype are given in Table IV. In the working bandwidth (9.1–9.6 GHz), the periodicity of the slots gives reason of a backward radiation in the $x-z$ plane, as in Fig. 7. Moreover to achieve a smooth transition from the PPW to the radiating slots the first three rows of slots have been designed with different length, as shown in Fig. 8.

While the procedure to derive the dispersion equation characterizing such a structure will not be given here, it is important to highlight the effect of the most significant geometrical parameters that affect the dispersion equation for propagation along the x direction, where the incident wave is traveling in the present case. These considerations will give approximate equations to predict the radiation properties of the slots in the $x-z$ plane.

TABLE IV
GEOMETRICAL DIMENSIONS IN MILLIMETERS OF THE SLOTS AND OF THE SUBSTRATE OF THE PARALLEL PLATE WAVEGUIDE

h	ϵ_r	l_{s1}	l_{s2}	l_{s3}	l_s	w_s	d_x	d_y
1.575	2.2	6	8	10	12	3.33	14	14

In particular the basic radiation mechanism is the following. In absence of the slots a q plane wave would propagate along the surface with real propagation constant k_{qTEM} essentially equal to $k_0\sqrt{\epsilon_r}$. When the $qTEM$ wave encounters the slot region, part of the energy reflects back in form of $qTEM$ plane wave and part progresses in the slotted waveguide region in form of leaky-wave. Since this $qTEM$ wave is a slow wave it does not directly radiate. However, the dominant -1 indexed LW of the Floquet mode expansion for periodic structures is given by

$$k_{x_{-1}} = k_{x_0} - \frac{2\pi}{d_x}. \tag{3}$$

It follows that the leaky wave beam angle can be approximated as

$$\theta \approx \arcsin\left(\frac{k_{x_0}(\omega) - \frac{2\pi}{d_x}}{k_0}\right). \tag{4}$$

In a first rough approximation the zero mode runs with the phase velocity of the incident wave, i.e.,

$$k_{x_0}(\omega) \approx k_0\sqrt{\epsilon_r}. \tag{5}$$

It is apparent from (4) that the beam pointing angle θ exhibits a variation versus frequency which is caused by the non linearity of $k_{x_{-1}}$ with frequency, also within the approximation condition (5). Furthermore, k_{x_0} has an intrinsic non linear dependence on ω, as shown in Fig. 9. There, the dispersion diagram in the Brillouin region is shown for an infinite array of slots with the geometry shown in the inset. We note from the zoom of Fig. 9(b) that the approximation (5) is not extremely accurate when compared with the results from HFSS [10] although, it could give an acceptable starting point in the design process. In any case the non-linearity of k_{x_0} with frequency is moderate thanks to the chosen low permittivity $\epsilon_r = 2.2$.

V. PROTOTYPE AND EXPERIMENTAL RESULTS

An antenna prototype has been built and measured. For any part of the antenna the dimensions given previously have been used. Moreover the number of radiating slot rows have been chosen to reduce the surface wave field at the last row of slots

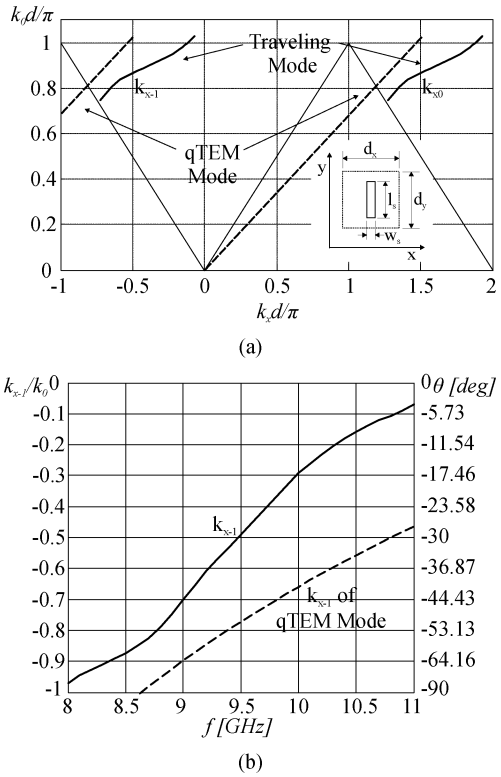

Fig. 9. (a) Brillouin dispersion diagram of the slots along the x direction. The dimensions of the unit cell depicted in the inset are given in Table IV. (b) Zoom of the region pertinent to the (-1) indexed backward mode in a $k-f$ graph.

to less than 1/10, indicating that 99% leaky-wave end point efficiency is achieved according to HFSS simulations [10]. The number of slot rows is 23. The antenna is shown in Fig. 10, its dimensions are 378×596 mm while the panel size where the antenna is built is 457×610 mm. The extremely low profile of the antenna, $h = 1.575$ mm, should be appreciated. The input reflection coefficient and the radiation patterns of the antenna have been measured. The directivity and gain of the complete structure have been calculated using the commercial tool Ansoft Designer [11] and a total efficiency of 81% is observed, that is mostly due to the residual spill-over losses.

The measured input reflection coefficient is shown in Fig. 11. The initial design of the antenna has been performed in the band range 9.1–9.6 GHz, with a central operative frequency of $f_c = 9.35$ GHz and a -10 dB relative bandwidth of $B_{rel} \approx 5.4\%$. The measured reflection coefficient has a -10 dB bandwidth in the range 8.85–9.65 GHz, with a resonance at $f_r \approx 9.136$ GHz. The small difference between f_r and f_c is $\Delta_f \approx 214$ MHz and it can be due to the tolerances of the fabrication process and of the material used. In particular for the dielectric a laminate Rogers RT/Duroid 5880 has been used. Anyway, the shift in frequency does not influence the operation of the antenna.

The variation of the main beam direction as a function of the frequency, typical of leaky wave antennas, has been investigated. The radiation patterns have been measured at $f = 9.1$ GHz; $f = 9.3$ GHz; $f = 9.6$ GHz, in the TNO far field range. The angle span used for the measurements is 180° with a step angle of 0.9°. The measured radiation patterns on the E-plane are reported in Fig. 12. Note that only the values

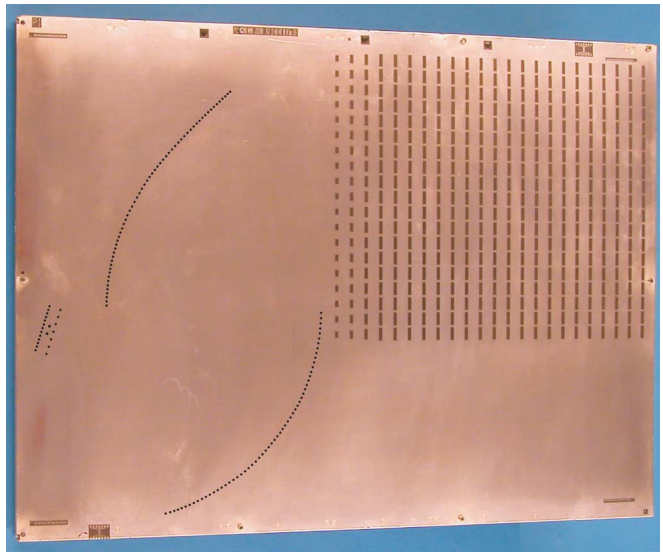

Fig. 10. Prototype of the antenna. The pins have been enhanced for better visibility.

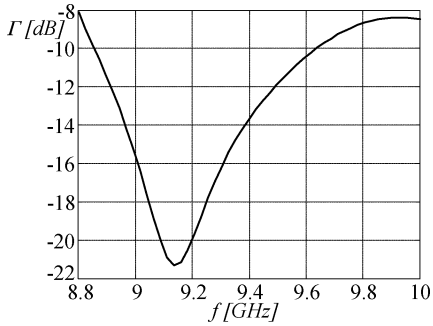

Fig. 11. Measured input reflection coefficient.

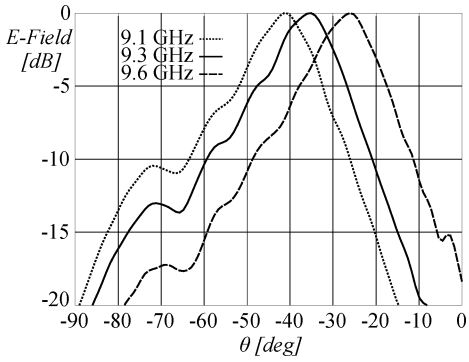

Fig. 12. Measured radiation patterns in the E-plane at different frequencies. θ is the usual elevation angle starting from the normal to the plane of the antenna.

for $-90° \leq \theta \leq 0°$ are reported since the radiation patterns are lower than -20 dB in the rest of the angle span. The antenna shows a frequency scanning behavior related to its leaky wave nature. In the frequency range considered a variation in pointing angle of $\triangle\theta \approx 15.3°$ is observed. The measured variation and pointing angle agree within less than 0.5° with the theoretical one given by (4) through the dispersion properties of the slot array of Fig. 9, as also reported in Table V.

Fig. 13 shows the measured radiation patterns on the E-plane and H-plane at the frequency $f = 9.3$ GHz. On the E-plane

TABLE V
POINTING ANGLE FROM THE MEASURED PATTERN (θ_m) AND THE DISPERSION DIAGRAM OF THE k_{x-1} OF FIG. 9(B) (θ_d)

$f(GHz)$	9.1	9.3	9.6
θ_m	$-41.4°$	$-35.1°$	$-26.1°$
θ_d	$-41°$	$-34.60°$	$-26.60°$

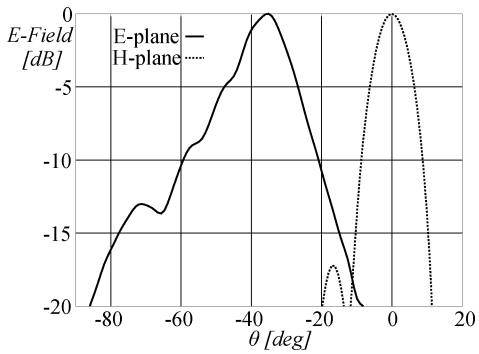

Fig. 13. Measured radiation patterns: electric field at the frequency (9.3 GHz) on the E-plane and H-plane. θ is the usual elevation angle starting from broadside for the E-plane and from the direction of maximum radiation for the H-plane.

we observed a 3-dB beamwidth of $BW \approx 12.6°$ and on the H-plane of $BW \approx 9.9°$. The patterns on these two planes could be shaped independently within a certain degree of freedom. In fact the pattern on the E-plane is dictated by the leaky wave contribution. In particular the 3-dB beamwidth is proportional to the attenuation constant of the leaky wave and the pointing angle is related to the propagation constant of the leaky wave. The pattern on the H-plane is linked to the dual reflector system and then to its physical dimensions and type of feeding.

Finally cross-polarization levels, always lower than -40 dB from cross to co-component maximum, are not reported for the sake of brevity.

VI. CONCLUSION

A dual offset Gregorian system exciting a planar leaky-wave antenna has been presented. The entire system is realized in PCB technology. The measured input reflection coefficient and radiation patterns have been presented and explained thanks to the dispersion properties of the structures and the characteristics of the dual reflector system. A pin-made feed, based on EBG concepts, has been used to feed the dual reflector system. The performances of the antenna are in perfect agreement with expectation and perfectly meet the frequency modulated-continuous wave (FMCW) Radar front-end requirements that drove the design. The FMCW Radar front end is operating from 9.1–9.6 GHz. This band is subdivided in five slots of 100 MHz each. Each slot corresponds to a different pointing direction and has sufficient bandwidth to recognize targets of a predefined dimension in a security application scenario. It is clear that lower dispersivity (with larger total bandwidth) would allow higher accuracy in tracking the targets and this will be the object of future investigations. The feed concept and the planar dual reflector system could be used in future planar imaging system applications, to achieve antennas with independent beams in the azimuth and elevation planes, resorting to frequency reuse and multiple focal plane feeds.

REFERENCES

[1] T. Zhao, D. R. Jackson, J. T. Williams, H. D. Yang, and A. A. Oliner, "2-D periodic leaky-wave antennas—Part I: Metal patch design," *IEEE Trans. Antennas Propag.*, vol. 53, pp. 3505–3514, Nov. 2005.
[2] T. Zhao, D. R. Jackson, and J. T. Williams, "2-D periodic leaky-wave antennas—Part II: Slot design," *IEEE Trans. Antennas Propag.*, vol. 53, pp. 3515–3524, Nov. 2005.
[3] Y. Mizuguchi, M. Akagawa, and H. Yokoi, "Offset Gregorian antenna," *Trans. Inst. Electron. Commun. Eng. Japan*, vol. 161-B, no. 3, pp. 166–173, Mar. 1978.
[4] Y. Mizugutch, M. Akagawa, and H. Yokoi, "Offset dual reflector antenna," in *IEEE Antennas Propag. Soc. Symp. Dig.*, Amherst, MA, Oct. 1976, pp. 2–5.
[5] Y. Rahmat-Samii, "Reflector antennas," in *Antenna Handbook*, Y. T. Lo and S. W. Lee, Eds. New York: Van Nostrand Reinhold, 1988.
[6] W. V. T. Rush, A. Prata, Y. Rahmat-Samii, and R. A. Shore, "Derivation and application of the equivalent paraboloid for classical offset Cassegrain and Gregorian antennas," *IEEE Trans. Antennas Propag.*, vol. 38, pp. 1141–1149, Aug. 1990.
[7] A. Neto, N. Llombart, G. Gerini, M. D. Bonnedal, and P. De Maagt, "EBG enhanced feeds for the improvement of the aperture efficiency of reflector antennas," *IEEE Trans. Antennas Propag.*, vol. 55, pp. 2185–2193, Aug. 2007.
[8] N. Llombart, A. Neto, G. Gerini, M. D. Bonnedal, and P. De Maagt, "Leaky wave enhanced feed arrays for the improvement of the edge of coverage gain in multibeam reflector antennas," *IEEE Trans. Antennas Propag.*, vol. 56, pp. 1280–1291, May 2008.
[9] N. Llombart, A. Neto, G. Gerini, and P. De Maagt, "Planar circularly symmetric EBG structures for reducing surface waves in printed antennas," *IEEE Trans. Antennas Propag.*, vol. 53, pp. 3210–3218, Oct. 2005.
[10] Ansoft HFSS10.0 ed. Ansoft Corporation, 1984–2007.
[11] Ansoft Designer3.0.0 ed. Ansoft Corporation, 1984–2007.

Mauro Ettorre (M'08) was born in Tricarico, Matera, Italy, in 1979. He received the Laurea degree (*summa cum laude*) in telecommunication engineering and the Ph.D. degree in electromagnetics from the University of Siena, Italy, in 2004 and 2008, respectively.

During his Laurea degree studies, he spent five months at the Technical University of Denmark (DTU), Lyngby, Denmark. Part of his Ph.D. was developed at the Defence, Security and Safety Institute of the Netherlands Organization for Applied Scientific Research (TNO), The Hague, The Netherlands, where he is currently working as an antenna researcher. His research interests include the analysis and design of leaky-wave antennas, periodic structures and electromagnetic band-gap structures.

Dr. Ettorre received the Young Antenna Engineer Prize during the 30th ESA Antenna Workshop 2008, in Noordwijk, the Netherlands.

Andrea Neto (M'00) received the Laurea degree (*summa cum laude*) in electronic engineering from the University of Florence, Florence, Italy, in 1994 and the Ph.D. degree in electromagnetics from the University of Siena, Siena, Italy, in 2000.

Part of his Ph.D. degree was developed at the European Space Agency Research and Technology Center, Noordwijk, The Netherlands, where he has been working for the antenna section for over two years. From 2000 to 2001, he was a Postdoc at the California Institute of Technology, Pasadena, working for the Sub-mm wave Advanced Technology Group. Since 2002, he is a Senior Antenna Scientist at TNO Defence, Security and Safety, Den Haag, The Netherlands. His research interests are in the analysis and design of antennas, with emphasis on arrays, dielectric lens antennas, wide band antennas and EBG structures. His research interests are in the analysis and design of antennas, with emphasis on arrays, dielectric lens antennas, wide band antennas and EBG structures.

Dr. Neto was a co-recipient of the 2008 H. A. Wheeler Applications Prize Paper Award from the IEEE Antennas and Propagation Society.

Giampiero Gerini (M'92–SM'08) received the M.S. degree (*summa cum laude*) and the Ph.D. in electronic engineering from the University of Ancona, Ancona, Italy, in 1988 and 1992. respectively.

From 1994 to 1997, he was Research Fellow at the European Space Research and Technology Centre (ESA-ESTEC), Nooordwijk, The Netherlands, where he joined the Radio Frequency System Division. Since 1997, he has been with the Netherlands Organization for Applied Scientific Research (TNO), The Hague, The Netherlands. At TNO Defence, Security and Safety, he is currently Chief Senior Scientist of the Antenna Unit in the Transceivers and Real-time Signal Processing Department. In 2007, he has been appointed as part-time Professor in the Faculty of Electrical Engineering, Eindhoven University of Technology, The Netherlands, with a Chair on Novel Structures and Concepts for Advanced Antennas. He is coauthor of four patents and more than 150 contributions to peer-reviewed journals, contribution to books and international conference proceedings. His main research interests are phased arrays antennas, electromagnetic bandgap structures, frequency selective surfaces and integrated antennas at microwave, millimeter and sub-millimeter wave frequencies. The main application fields of interest are radar, space and telecommunication systems.

Dr. Gerini was a co-recipient of the 2008 H. A. Wheeler Applications Prize Paper Award from the IEEE Antennas and Propagation Society.

Stefano Maci (M'92–SM'99–F'04) was born in Rome, Italy, in 1961. He received the Laurea degree (*cum laude*) in electronic engineering from the University of Florence, Italy, in 1987.

Since 1998, he has been with the University of Siena, Italy, where he presently is a Full Professor. He was a coauthor of an incremental theory of diffraction for the description of a wide class of electromagnetic scattering phenomena at high frequency, and of a diffraction theory for the high frequency analysis of large truncated periodic structures. His research interests include the theory of electromagnetism, integral equation methods, large phased array antennas, planar antennas and multilayer structures, reflector antennas and feed horns, metamaterials. In 2004, he was the Founder and is presently the Coordinator of the "European School of Antennas" (ESoA), a post graduate school comprising 26 courses and about 150 teachers from 20 European research centers. He was responsible for several projects funded by the European Union (EU), the European Space Agency (ESA-ESTEC), and various European industries. He was Work Package Leader in the Network of Excellence "Antenna Center of Excellence" (FP6, EU). He is principal author or coauthor of about 100 papers published in international journals, eight book chapters, and about 300 papers in proceedings of international conferences.

Prof. Maci was the recipient of several Best Paper Awards presented at international conferences. He was previously a member of the Technical Advisory Board of the International Scientific Radio Union (URSI) Commission B and Convenor in a URSI General Assembly. He was the Coordinator of the advisory board of the Italian Ph.D. school of Electromagnetism. He is a member of the Delegate Assembly of the European Association of Antennas and Propagation, of a NATO panel on metamaterials and MEMS, and a member of the scientific board of the Italian Society of Electromagnetism (SIEM). He has been an invited speaker at many international conferences, and presenter of various short courses about EBG material, high-frequency methods, and computational methods. He served as an Associate Editor of the IEEE TRANSACTIONS ON ELECTROMAGNETIC COMPATIBILITY from 1999 to 2001. He is presently as Associate Editor of the IEEE TRANSACTIONS ON ANTENNAS AND PROPAGATION and was Guest Editor of two Special Issues.